



Featured Article

Longitudinal uncoupling of cerebral perfusion, glucose metabolism, and tau deposition in Alzheimer's disease

Antoine Leuzy^a, Elena Rodriguez-Vieitez^a, Laure Saint-Aubert^a, Konstantinos Chiotis^a,
Ove Almkvist^{a,b,c}, Irina Savitcheva^d, My Jonasson^{e,f}, Mark Lubberink^{e,f}, Anders Wall^{e,g},
Gunnar Antoni^g, Agneta Nordberg^{a,b,*}

^aDivision of Translational Alzheimer Neurobiology, Department of Neurobiology, Care Sciences, and Society, Karolinska Institutet, Stockholm, Sweden

^bDepartment of Geriatric Medicine, Karolinska University Hospital, Huddinge, Sweden

^cDepartment of Psychology, Stockholm University, Stockholm, Sweden

^dDepartment of Radiology, Karolinska University Hospital, Huddinge, Sweden

^eRadiology, Department of Surgical Sciences, Uppsala University, Uppsala, Sweden

^fDepartment of Medical Physics, Uppsala University Hospital, Uppsala, Sweden

^gDepartment of Medicinal Chemistry, Uppsala University, Uppsala, Sweden

Abstract

Introduction: Cross-sectional findings using the tau tracer [¹⁸F]THK5317 (THK5317) have shown that [¹⁸F]fluorodeoxyglucose (FDG) positron emission tomography (PET) data can be approximated using perfusion measures (early-frame standardized uptake value ratio; ratio of tracer delivery in target to reference regions). In this way, a single PET study can provide both functional and molecular information.

Methods: We included 16 patients with Alzheimer's disease who completed follow-up THK5317 and FDG studies 17 months after baseline investigations. Linear mixed-effects models and annual percentage change maps were used to examine longitudinal change.

Results: Limited spatial overlap was observed between areas showing declines in THK5317 perfusion measures and FDG. Minimal overlap was seen between areas showing functional change and those showing increased retention of THK5317.

Discussion: Our findings suggest a spatiotemporal offset between functional changes and tau pathology and a partial uncoupling between perfusion and metabolism, possibly as a function of Alzheimer's disease severity.

© 2017 The Authors. Published by Elsevier Inc. on behalf of the Alzheimer's Association. This is an open access article under the CC BY-NC-ND license (<http://creativecommons.org/licenses/by-nc-nd/4.0/>).

Keywords:

Positron emission tomography (PET); Tau imaging; THK5317; Neurofibrillary tangles; FDG; Hypometabolism; Perfusion imaging; R₁; Perfusion SUVR; Alzheimer's disease; Prodromal Alzheimer's disease; Alzheimer's disease dementia; Mild cognitive impairment; Longitudinal study

1. Introduction

In addition to amyloid β (A β) and tau pathology, Alzheimer's disease (AD) is characterized by decreased brain perfusion [1,2] and glucose metabolism [3,4]. Cross-sectional

comparative studies have indeed shown regional perfusion and metabolism to be tightly coupled in neurodegenerative disorders, including AD [5,6], and in controls, under both active and resting physiological conditions [7]. As such, [¹⁸F]fluorodeoxyglucose (FDG) positron emission tomography (PET) metabolic data can be approximated using early-frame standardized uptake value ratio (p-SUVR) and the ratio of tracer delivery in target and reference regions (R₁), measures shown to correlate strongly with brain perfusion [8,9].

*Corresponding author. Tel.: +46 8 585 85467; Fax: +46 8 585 85470.
E-mail address: agneta.k.nordberg@ki.se

Comprehensive compartmental approaches, involving the solution of differential equations and requiring arterial blood sampling, form the basis of PET-based estimation of physiological parameters of interest [10]. Reduced configuration models have been developed, however, whereby the input function derived from arterial plasma is replaced by that from a reference region [10]. These approaches obviate the need for arterial cannulation and metabolite assay, simplifying scanning protocols and data analysis procedures. While the objective of these models is to obtain an estimate of tracer binding, such as the distribution volume ratio (DVR)—total distribution volume in target over reference region—derived from reference Logan, a graphical approach involving linearization [11], perfusion information in the form of R_1 can also be obtained using models that rely on iterative curve fitting such as the simplified reference tissue model [12] and related approaches involving parameter coupling [13]. By contrast, calculation of p-SUVR does not require kinetic modeling and instead reflects the assumption that early-time frame uptake reflects tracer delivery [14], with p-SUVR thus reflective of R_1 .

Findings from studies implementing the use of perfusion measures (p-SUVR and R_1) with $A\beta$ PET tracers have been shown to closely correlate with FDG, and to carry potential clinical utility, having been used to distinguish AD from controls [15], frontotemporal lobar degeneration [16], and cerebral amyloid angiopathy [17]. Findings from our earlier cross-sectional study using the tau-specific PET tracer [^{18}F]THK5317 (THK5317) [18,19] in AD suggest that tau imaging may also prove able to provide both molecular and functional information [9], similar to that proposed for $A\beta$ PET [16]. Given the possible future clinical use of tau PET for diagnostic purposes and evaluation of drug therapies, as well as the advantages inherent to dual-use imaging [20,21], further exploration of these findings is warranted.

In this study, we sought to quantify the longitudinal relationship between THK5317 perfusion measures, glucose metabolism (FDG SUVR), and tau pathology (THK5317 DVR), in a cohort of patients with AD. The test-retest reproducibility of THK5317 perfusion measures was likewise investigated.

2. Methods

2.1. Participants

Sixteen AD patients (10 prodromal AD and six AD dementia) who had previously participated in baseline investigations [22,23] were here followed up after a median interval of 17 months (interquartile range: 15–18 months) [24]. All patients had originally undergone clinical assessment for memory problems at the Department of Geriatric Medicine, Karolinska University Hospital Huddinge, Stockholm, Sweden, and had been followed up after diagnosis, as detailed elsewhere [22]. Patients diagnosed with AD dementia met the revised NINCDS-ADRDA criteria for probable AD and

showed in vivo evidence of AD pathology (abnormal [^{11}C] Pittsburgh Compound B [PIB]) [25]. Patients who fulfilled the diagnosis of mild cognitive impairment [26] and showed a positive PIB scan were diagnosed as prodromal AD [27].

All subjects provided informed consent to take part in the present study, which was conducted according to the Declaration of Helsinki and subsequent revisions. Ethical approval was obtained from the regional human ethics committee of Stockholm and the Faculty of Medicine and Radiation Hazard Ethics Committee of Uppsala University Hospital, Uppsala, Sweden.

2.2. Acquisition and analysis of imaging data

Dynamic THK5317 studies were conducted over 60 minutes, following intravenous bolus injection of 217 ± 42 MBq. A static 15-minute FDG scan was performed 30 minutes after injection of 3 MBq/kg. Dynamic baseline and follow-up THK5317 and FDG PET images were coregistered to their respective T1-MRIs using PMOD (v.3.5; PMOD Technologies Ltd., Zurich, Switzerland). Structural images were segmented using SPM8, with the inverse transformation parameters generated used to spatially warp a probabilistic atlas [28] into native T1 image space. Voxelwise THK5317 p-SUVR and simplified reference tissue model R_1 maps were obtained with PMOD, using the cerebellar cortex as reference tissue [9,12]. For p-SUVR, the interval 0–3 minutes was selected based on the previously reported observation that this interval showed the highest correlations with FDG [9]. Parametric SUVR (30–45 minutes) and Logan DVR images (30–60 minutes) were created for FDG and THK5317, respectively, using the cerebellar cortex as reference region [11,22].

Annual percentage change was calculated voxelwise for all PET parameters as follows: $\{[(\text{Follow-up} - \text{Baseline}) / \text{Baseline}] / \text{Time interval between scans (years)}\} \times 100\%$. In order to examine the spatial overlap of resulting parametric maps, the latter were binarized using the average isocortical test-retest reproducibility of THK5317 p-SUVR and R_1 (rounded up to 3%), thereby excluding voxels within the test-retest repeatability range of perfusion measures. Voxelwise THK5317 p-SUVR, R_1 , and FDG SUVR maps were used to perform pairwise correlations using the biological parametric mapping software package (MATLAB v.3.3). An 8-mm filter and an a priori gray matter mask were then applied to spatially normalized PET images with resulting correlation maps thresholded at $P < .001$ (uncorrected, cluster extent ≥ 20 voxels).

2.3. Test-retest reproducibility of THK5317 perfusion measures

To establish the test-retest reproducibility of THK5317 p-SUVR and R_1 , five subjects (four prodromal AD and one possible corticobasal syndrome) [29] underwent a retest THK5317 PET scan (range: 13–37 days).

Table 1
Longitudinal regional PET measures

	Medial temporal	Lateral temporal	Frontal	Parietal	Posterior cingulate	Occipital	Isocortical composite
THK5317 p-SUVR							
Baseline	0.81 (0.75–0.90)	0.90 (0.84–0.96)	0.94 (0.88–0.97)	0.90 (0.83–0.98)	1.04 (0.98–1.11)	0.99 (0.93–1.07)	0.94 (0.87–0.98)
Follow-up	0.78 (0.76–0.87) [‡]	0.86 (0.81–0.94) [‡]	0.90 (0.87–0.98)*	0.86 (0.81–0.92) [‡]	0.98 (0.94–1.07) [‡]	0.95 (0.90–1.02)	0.90 (0.86–0.96)*
THK5317 R ₁							
Baseline	0.78 (0.71–0.87)	0.86 (0.79–0.92)	0.90 (0.86–0.94)	0.86 (0.81–0.95)	0.96 (0.94–1.03)	0.98 (0.92–1.09)	0.91 (0.94–0.96)
Follow-up	0.75 (0.72–0.83)*	0.81 (0.76–0.88) [‡]	0.87 (0.83–0.96)*	0.83 (0.76–0.92) [‡]	0.93 (0.87–1.03)*	0.97 (0.87–1.02) [‡]	0.86 (0.82–0.95)*
FDG SUVR							
Baseline	0.88 (0.82–0.92)	0.99 (0.98–1.05)	1.12 (1.05–1.16)	1.07 (0.99–1.10)	1.14 (1.10–1.21)	1.15 (1.09–1.18)	1.07 (1.04–1.14)
Follow-up	0.86 (0.80–0.91) [‡]	0.96 (0.91–1.03)*	1.09 (1.03–1.16)	1.04 (0.93–1.10)*	1.14 (1.02–1.19) [‡]	1.13 (1.09–1.21)*	1.06 (0.99–1.12)
THK5317 DVR							
Baseline	1.22 (1.17–1.26)	1.20 (1.16–1.23)	1.14 (1.13–1.22)	1.18 (1.11–1.20)	1.29 (1.24–1.35)	1.20 (1.13–1.22)	1.18 (1.13–1.21)
Follow-up	1.21 (1.16–1.25)	1.20 (1.14–1.22)	1.14 (1.11–1.21)	1.17 (1.12–1.22)	1.28 (1.25–1.35)	1.18 (1.13–1.22)	1.18 (1.12–1.23)

Abbreviations: DVR, distribution volume ratio; FDG, [¹⁸F]fluorodeoxyglucose; PET, positron emission tomography; p-SUVR, early-frame standardized uptake value ratio; R₁, ratio of tracer delivery in target to reference region; ROI, region of interest; THK5317, [¹⁸F]THK5317.

NOTE. Linear mixed-effects models were used to assess changes between baseline and follow-up data for each PET measure (THK5317 p-SUVR, R₁, DVR, and FDG SUVR) within ROIs, using the following equation: $PET\ measure_{ROI} = \beta_0 + \beta_1 (Time\ point) + Random\ intercept(i) + \epsilon$, where β_0 and β_1 are fixed-effects coefficients, $Time\ point$ is a fixed-effects nominal variable (baseline and follow-up examinations), and $Random\ intercept$ is a variable that takes into account the individual subject number, i , with the error term represented by ϵ .

*Significantly lower than baseline, $P < .05$.

[‡]Significantly lower than baseline, $P < .01$.

[‡]Trend-level significance for decrease from baseline.

2.4. Statistical methods

Analyses were performed using R (v.3.3.3; R Foundation for Statistical Computing, <https://www.R-project.org/>), with $P < .05$ (two-tailed) used to indicate statistical significance. Patient characteristics at baseline and follow-up were compared using Mann Whitney U and Fisher exact tests. Intra-subject test (T)-retest (R) variability of THK5317 perfusion measures was assessed within each region of interest (ROI), using both the relative $\{[(R - T)/(T)] \times 100\%$ and absolute $\{[|(R - T)/0.5(R + T)]| \times 100\%$ difference between scans. Cross sectional associations between THK5317 perfusion measures and FDG, and between THK5317 p-SUVR and R₁, were assessed across all subjects using a nested design with linear regression and Pearson's correlation coefficient. Given previous studies showing that brain perfusion can be affected by age, sex, education level, and apolipoprotein E (*APOE*) $\epsilon 4$ genotype [30–33], partial correlation analyses accounting for these variables were also performed within individual ROIs.

Linear mixed-effects models (LMMs), including random intercepts at the subject level, were used to assess longitudinal changes in PET measures (see Table 1 legend for equation) and the regional longitudinal associations between pairs of PET measures (see Supplementary Table 4 legend for equations). LMMs were also used to assess, in an exploratory manner, whether the longitudinal change in the different PET measures differed between diagnostic groups. To that end, a separate LMM was used to assess each PET measure as a dependent variable, with time point (baseline and follow-up investigations), diagnostic groups (prodromal versus AD dementia), and the interaction between the two as fixed factors, allowing for random intercepts across different

patients and ROIs, using a nested design (see Supplementary Table 5 legend for equations).

3. Results

3.1. Subject characteristics

Patient demographic and clinical characteristics are presented in Table 2. No group differences were found for age, sex, education, or for the percentage of subjects carrying the *APOE* $\epsilon 4$ allele. At both baseline and follow-up, Mini-Mental State Examination scores were significantly lower in the AD dementia group, relative to prodromal AD group ($P < .05$). In the entire sample, Mini-Mental State Examination scores were significantly lower at follow up, relative to baseline ($P < .05$).

3.2. Test-retest reproducibility of THK5317 perfusion measures

Intra-subject variability was low for both p-SUVR and R₁ (Supplementary Tables 1 and 2), similar to those previously reported for THK5317 DVR values [22]. Across subjects, the test-retest variation for p-SUVR ranged from 2.41% (frontal cortex) to 6.28% (occipital cortex), with an isocortical repeatability value of 2.43%. Similar results were obtained for R₁ (range: 2.59% [frontal cortex] to 6.03% [occipital cortex]; isocortical repeatability of 3.13%).

3.3. Regional longitudinal changes in THK5317 perfusion measures, FDG SUVR, and THK5317 DVR

Baseline and follow-up values for THK5317 (perfusion measures and DVR) and FDG SUVR are reported in Table 1. Across all subjects, perfusion measure values declined

Table 2
Demographic and clinical characteristics within and across diagnostic groups

	Prodromal AD	AD dementia	All patients
N	10	6	16
Age at baseline (years)	65.0 (69.0:74.0)	68.5 (64.8:73.0)	70.5 (66.0:76.0)
Gender (male/female)	4/6	1/5	5/11
Education (years)	12.0 (10.3–13.8)	14.5 (13.3–15.8)	13.0 (12.0–15.3)
<i>APOE</i> ϵ 4 (carriers/noncarriers)	6/3*	5/1	11/4*
MMSE at baseline	28 (27–30) [†]	23.5 (23–24.8) [§]	26 (23–28.5) [‡]
MMSE at follow-up	26 (25–27) [†]	20 (16.3–23.8) [§]	25 (23.5–26.5) ^{‡,¶}
PIB status (positive/negative)	10/0	6/0	16/0

Abbreviations: AD, Alzheimer's disease; *APOE* ϵ 4, apolipoprotein ϵ 4 allele; MMSE, Mini-Mental State Examination; PIB, [¹¹C]Pittsburgh Compound (B). NOTE. Data presented as medians (range) or as N.

*Data missing for one subject.

[†]Data reported for nine patients who completed both baseline and follow-up investigations.

[‡]Data reported for fifteen patients who completed both baseline and follow-up investigations.

[§]Significantly lower, relative to prodromal AD ($P > .05$).

[¶]Significantly lower, relative to baseline ($P > .05$).

significantly in lateral temporal, frontal, parietal, and composite isocortical regions. Within medial temporal and posterior cingulate ROIs, however, p-SUVR and R_1 differed with significant and trend-level findings, respectively. In contrast to perfusion measures, declines in metabolism reached significance only in lateral temporal, parietal, and occipital regions. Strong correlations between perfusion measures and metabolism were observed at both time points (Fig. 1, uncorrected for age, sex, education, and *APOE* ϵ 4; Supplementary Fig. 1 and Supplementary Table 3 in comparison to adjustment for covariates). Correlational analysis by subgroup, however, showed that while the correlation coefficients between perfusion measures and metabolism were above 0.90 at both time points in AD dementia, those for prodromal AD were weaker at both time points and showed increases from baseline (p-SUVR and FDG, 0.64–0.77, $P < .001$; R_1 and FDG, 0.70–0.79, $P < .001$). The longitudinal pairwise associations between perfusion measures and metabolic imaging, as well as between p-SUVR and R_1 , were significant across all ROIs (Supplementary Table 4). No significant longitudinal increases in regional DVR values were noted.

3.4. Voxel-based annual percentage change and spatial overlap of THK5317 perfusion measures, FDG SUVR, and THK5317 DVR

Figs. 2 and 3 show, respectively, surface projection images of group-level averages (baseline and follow-up) and voxelwise annual percentage change for perfusion measures (Figs. 2A, 2B, 3A and 3B), metabolism (Figs. 2C and 3C), and tau (Figs. 2D and 3D). For THK5317 perfusion measures, a similar pattern of change was observed in lateral temporal and parietal regions. Medially, however, areas of change differed between parameters, with p-SUVR-specific clusters noted in cingulate, prefrontal, and orbitofrontal cortices. Despite a resemblance with respect to more posterior brain regions, the extent of change was also greater for p-SUVR in the precuneus and the superior aspect of the cuneus. Changes

in metabolism, predominant in prefrontal, temporal, and medial parietal regions showed greater correspondence with declines in p-SUVR, relative to R_1 . Focal increases in THK5317 retention were found in the orbitofrontal gyrus, dorsolateral prefrontal cortex, temporal cortex, and occipital cortex.

Fig. 3 also shows the spatial overlap between binarized annual percentage change maps for perfusion measures (Fig. 3E), for perfusion measures and metabolism (Fig. 3F and G), and for p-SUVR and tau (Fig. 3H). Overlap between declines in each perfusion measure was concentrated primarily in the posterior cingulate and lateral parietal cortex, lateral temporal cortex, including anterior poles, medial aspects of the inferior temporal lobe, and frontotemporal operculum. Comparison of overlap patterns between perfusion measures and annual declines in FDG showed a pattern suggestive of greater temporoparietal overlap with R_1 , with more frontal predominant overlap for p-SUVR. Overlap between perfusion measures and annual increase in THK5317 DVR was confined to the medial temporal lobe.

3.5. Effect of diagnostic groups on the longitudinal change in THK5317 perfusion measures, FDG SUVR, and THK5317 DVR

Findings from LMM analyses examining whether there were differences between diagnostic groups (prodromal AD and AD dementia) with respect to the longitudinal change in the different PET measures here investigated are reported in Supplementary Table 5. For longitudinal metabolism, there was a significant interaction between time point and diagnostic group, in that the decline between time points was greater for the AD dementia group, relative to prodromal AD (Supplementary Fig. 2). In contrast, this interaction term was not significant for perfusion measures or tau.

Fig. 4 shows subgroup-level surface projection images of voxelwise annual percentage change for perfusion

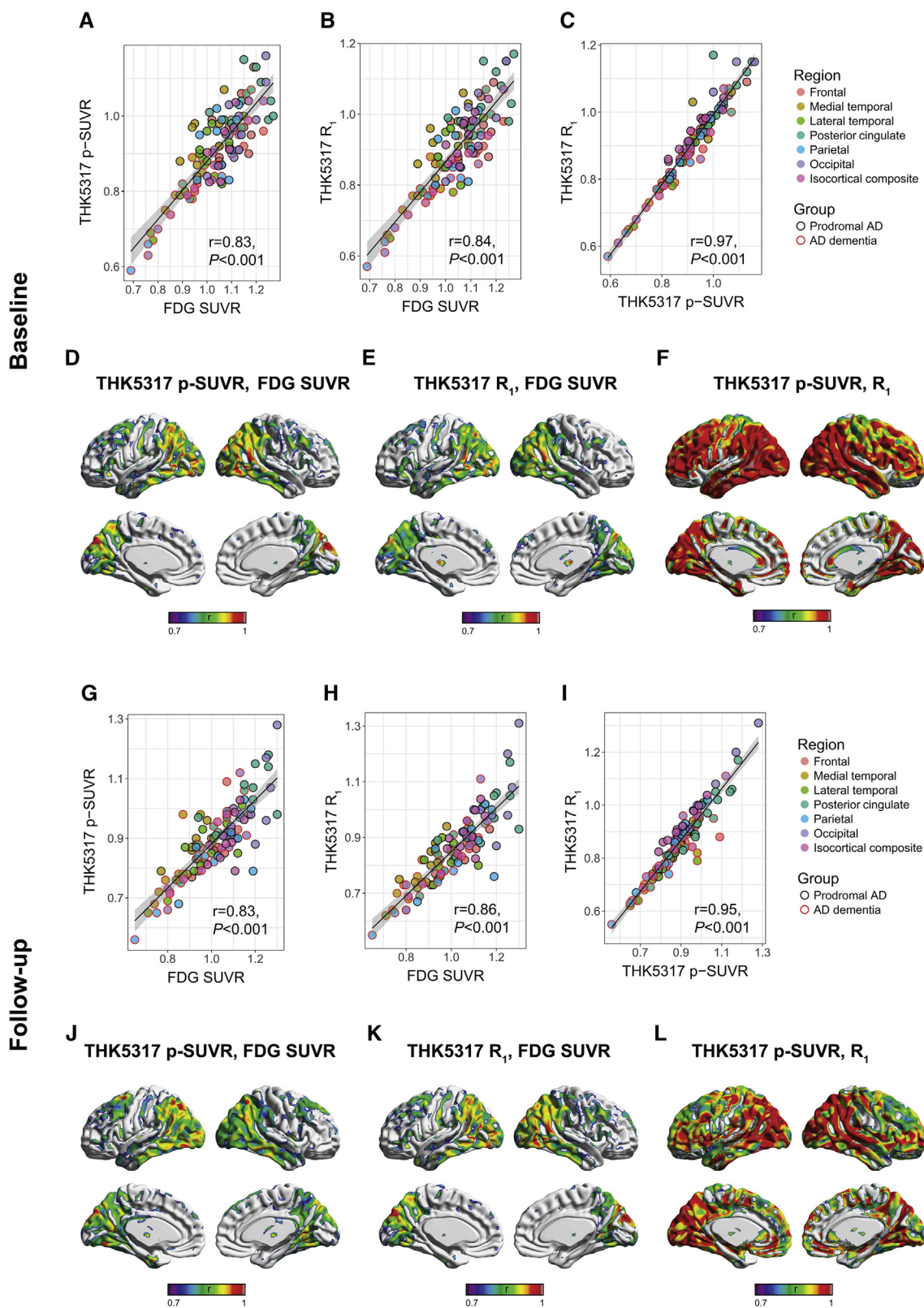


Fig. 1. Linear regression plots and voxelwise maps showing the relationship between THK5317 perfusion measures and glucose metabolism at baseline and follow-up. Regional correlations between THK5317 p-SUVR and FDG SUVR, THK5317 R_1 and FDG SUVR, and between THK5317 perfusion measures at baseline are shown in (A, B, and C), respectively. Regional correlations for the same pairings at follow-up are shown in (G, H, and I). Voxelwise correlations are shown in (D–F) and (J–L). Abbreviations: FDG, [^{18}F]fluorodeoxyglucose; p-SUVR, early-frame standardized uptake value ratio; R_1 , ratio of tracer delivery in target to reference region; THK5317, [^{18}F]THK5317.

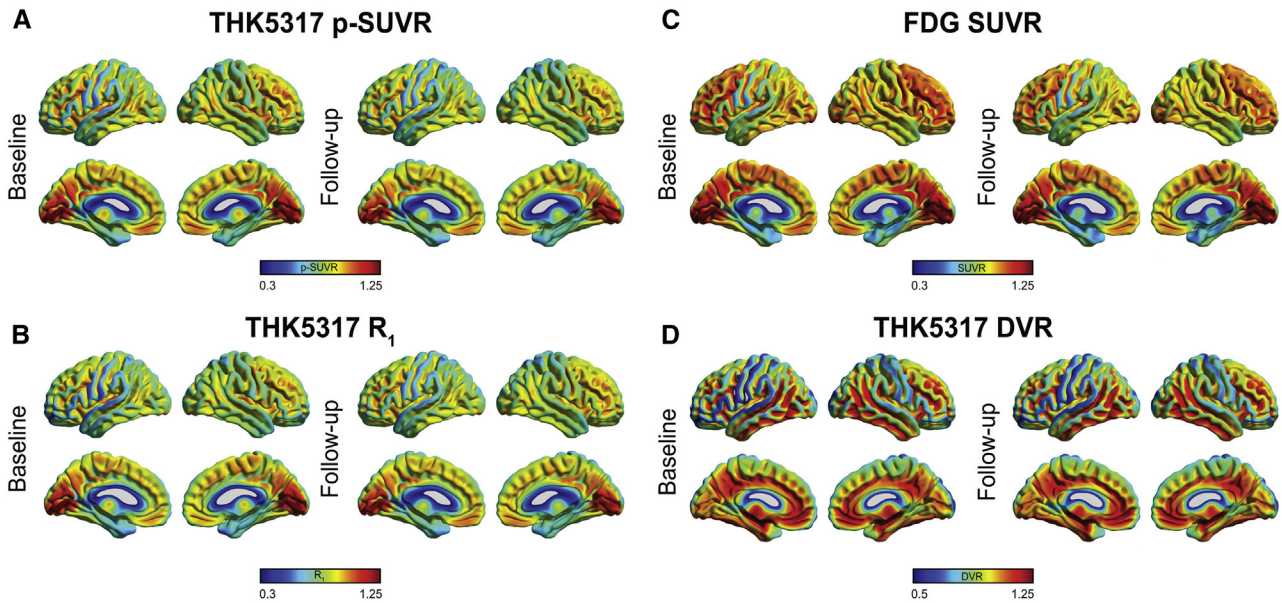


Fig. 2. Group-level average maps, at baseline (top row) and follow-up (bottom row), for THK5317 p-SUVR (A), THK5317 R₁ (B), FDG SUVR (C), and THK5317 DVR (D). Abbreviations: DVR, distribution volume ratio; FDG, [¹⁸F]fluorodeoxyglucose; p-SUVR, early-frame standardized uptake value ratio; R₁, ratio of tracer delivery in target to reference region; THK5317, [¹⁸F]THK5317.

measures (Fig. 4A and B), metabolism (Fig. 4C), and tau (Fig. 4D). In contrast to prodromal AD patients, where perfusion measures mirrored one another, p-SUVR and R₁ showed incomplete spatial overlap in AD dementia patients; both parameters also showed greater change in this group. Between-group differences were marked for FDG, with widespread declines in the AD dementia group contrasting with a more focal pattern of change in prodromal AD patients. Both prodromal AD and AD dementia patients, however, showed focally-increased THK5317 retention within cuneal, inferior temporal, and anterior frontal areas, with AD dementia patients in addition showing increases in dorsolateral prefrontal areas. Using binarized annual percentage change images, the greater spatial overlap between THK5317 perfusion measures can be appreciated in Fig. 4E, as can the superior spatial overlap between perfusion measures and metabolism in AD dementia patients (Fig. 4F and G). Although relatively modest in size, an overlap between perfusion and tau was observed in basal temporal areas across groups (Fig. 4H).

4. Discussion

In light of the growing use of tau PET imaging and the high cost of FDG investigations [34], perfusion measures derived from a tau PET scan stand as an attractive alternative, allowing for the circumvention of serial imaging and the lowering of costs, patient discomfort, and radiation exposure. In the present longitudinal study, perfusion measures were derived from dynamic THK5317 PET studies and compared to FDG PET and THK5317 DVR. THK5317

perfusion measures showed low intrasubject variability and test-retest reproducibility below 3% across isocortical regions, supporting their potential use in clinical settings. Application of LMMs showed good regional agreement between declines in perfusion measures and metabolism over the 17-month follow-up period; no significant increases were found for tau, however. Despite strong correlations at follow-up, similar to those previously reported using baseline data [9], voxelwise annual percentage change maps for perfusion and metabolism showed only partial spatial overlap. Exploratory analysis of the effect of diagnostic group on the longitudinal change in perfusion, metabolism, and tau pathology showed a significant effect for the interaction between time point (baseline and follow-up) and diagnostic group for FDG, in that the decline in SUVR was greater for the AD dementia group, relative to prodromal AD. Subsequent subgroup-level voxelwise analyses showed that the spatial overlap between the longitudinal changes in perfusion and metabolism was most divergent in the prodromal AD group, with the overlap between changes in perfusion and tau confined to basal medial temporal areas across both subgroups.

The group-level regional declines in perfusion measures and glucose metabolism herein observed align well with findings reported in previous longitudinal studies in AD using comparable follow-up durations [35,36]. The incomplete spatial overlap between voxel-level annual change findings, however, suggests a partial loss of parallelism between perfusion and metabolism, most prominently at the prodromal AD stage. The lower correlations between perfusion measures and FDG at baseline in prodromal AD patients, and their increase in strength

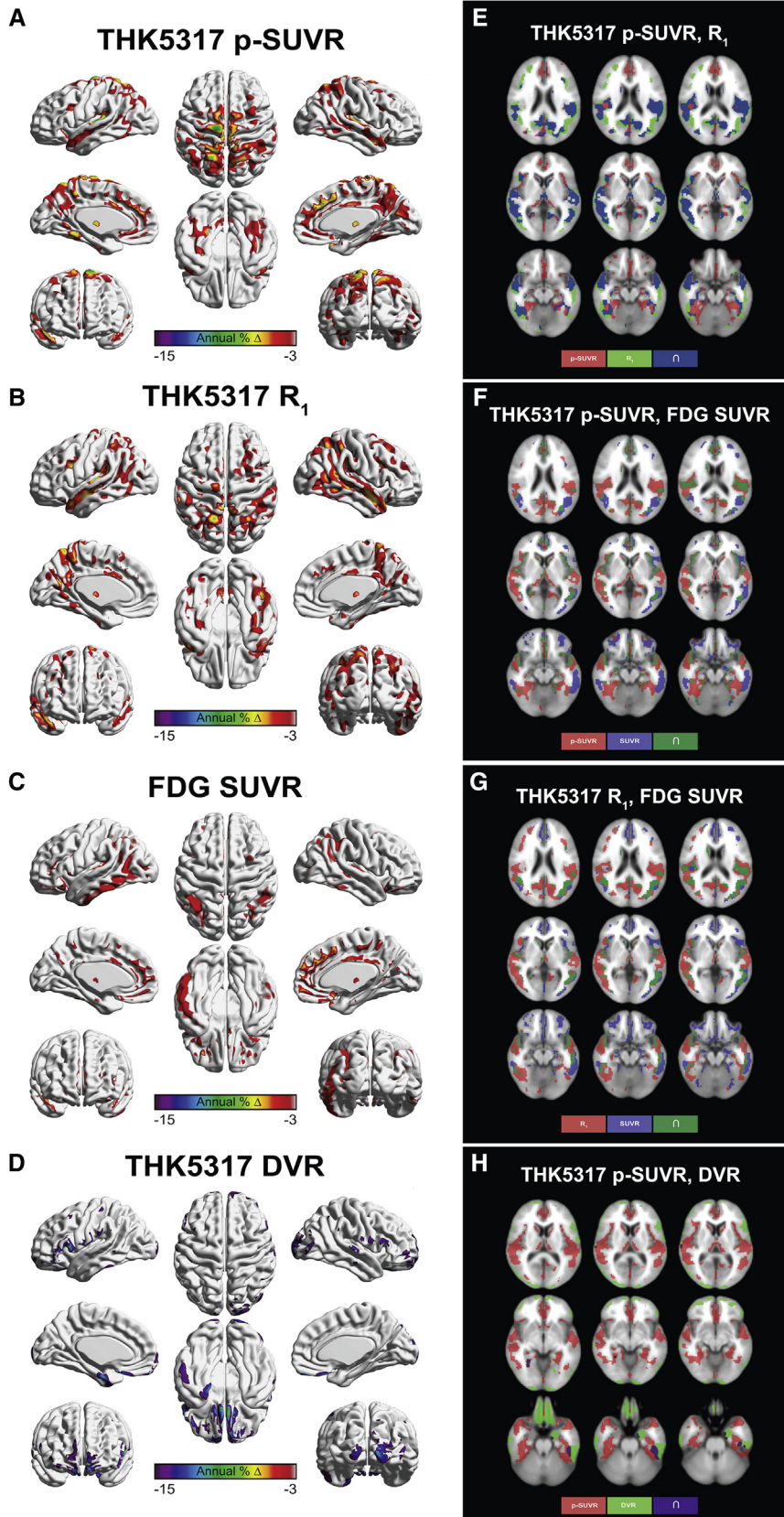


Fig. 3. Group-level annual percentage change maps for perfusion, metabolism, and tau. Annual percentage change for each PET measure was created for each subject as follows: $\{[(\text{Follow-up} - \text{Baseline})/\text{Baseline}]/\text{Time interval between scans (years)}\} \times 100\%$. Surface projection images showing annual percentage change for THK5317 p-SUVR (A), THK5317 R₁ (B), FDG SUVR (C), and THK5317 DVR (D). Spatial overlap of annual percentage change images binarized

longitudinally, lend support to this hypothesis and align with longitudinal findings using PIB p-SUVR [37]. Although the temporal ordering of changes in perfusion and metabolism cannot be specifically addressed by our findings, given the comparatively closer association between changes in perfusion and metabolism here observed in the AD dementia group, it may be that an acceleration in the decline in metabolism is specific to the dementia phase of AD. It could then be speculated that an acceleration in the decline of perfusion may then occur in more advanced AD dementia, or that, alternatively, perfusion follows a more or less continuous pattern of decline across the symptomatic stages of AD.

The precise mechanisms governing the dissociation between perfusion and metabolism here observed are as yet unclear. Although A β and tau have been shown to act in concert to induce and potentiate synaptic damage, as reflected by reduced glucose metabolism [38,39], and to alter brain perfusion via effects on cerebral arteries and microvasculature [40], these processes may progress according to differing scales such that, while evolving in parallel, the magnitude of changes in brain perfusion may supersede that of glucose metabolism in the prodromal stage of AD. The higher alignment of changes in perfusion and metabolism in AD dementia patients may then reflect the cumulative effects of these processes, a scenario strengthened by the known downstream effects of A β and the observation that its deposition continues through mild-to-moderate AD [41]. The finding of increased glial activation in prodromal AD has also recently been hypothesized to exert a protective effect, likely via clearance of A β and tau [42,43]. The loss of this protective phenotype with disease progression may coincide with the significant decline in glucose metabolism we observed in AD dementia subjects. Glial activation is also reported to potentially contribute to increases in metabolism [44], and thus a possible increase in glial activation in the prodromal stage of AD may be responsible for the observed attenuation in metabolic decline [45].

The lack of significant regional increases in THK5317 DVR may reflect within group heterogeneity and consequently high between-group overlap in regional tau burden and rates of change. A recent longitudinal study that focused on changes in tau pathology and metabolism using the same study population indeed showed that regional tau load and patterns of propagation differed substantially across patients, suggesting that patients were at differing neuropathological stages

with respect to tau pathology, despite the same diagnostic classification [24]. Furthermore, tau propagation at a group level did not relate to metabolism, which was found to decrease in a homogeneous fashion [24]. Voxelwise, however, we identified areas displaying increases in THK5317 in regions consistent with Braak stages V/VI [46]; similar patterns of increase were found between subgroups. The relative absence of overlap between declining perfusion and increases in tau suggests a lag phase between these processes [24]. Interestingly, comparison of overlap findings between subgroups showed that the increase in overlap between groups was due to the expansion of the cluster for perfusion and not of tau.

The significance of discrepancies between perfusion measures is considerable given the favorability of p-SUVR in clinical settings due the fact that, unlike R₁, it does not require dynamic imaging. Voxelwise maps for annual change in perfusion measures showed that these discrepancies were predominant in the AD dementia group. A possible reason for the overall discrepancy may be that p-SUVR represents a cruder estimate of brain perfusion than R₁ because it includes signal from early binding to tau aggregates. Areas showing greater decline with p-SUVR, relative to R₁, however, did not overlap with areas showing increased THK5317 DVR. This finding may thus relate to the lower percentage value we adopted for thresholding, as previous longitudinal findings using the same tau tracer showed annual percentage change in tau below our threshold in AD patients more advanced than those here included [47]. Alternatively, these inconsistencies may relate to differences in measurement variability as p-SUVR is derived from two independent parameter estimates while R₁ is derived directly as a single parameter [8]. Although the variance (interquartile range) we observed between measures was indeed higher for p-SUVR isocortically, this pattern was not present across all ROIs. While there have to date been no studies addressing the longitudinal relationship between p-SUVR and R₁ using tau PET tracers, it may be that their suitability, in terms of coupling to one another and to glucose metabolism, may vary as a function of disease severity and, possibly, brain region.

Certain methodological aspects, however, limit the interpretation of our findings. In addition to the comparatively short follow-up time and variability in clinical progression across patients, the relatively limited sample size did not allow for detailed comparison of prodromal and AD dementia groups using inferential statistics. Such analyses would likely have provided additional information on the interrelationship between the measures here investigated. Furthermore, nonlinear

using the average test-retest repeatability of THK5317 perfusion measures is shown for THK5317 perfusion measures (E), THK5317 p-SUVR and FDG SUVR (F), and THK5317 R₁ and FDG SUVR (G). For the overlap between perfusion and THK5317 DVR (H), THK5317 p-SUVR was chosen because of the potentially greater clinical applicability of p-SUVR due the fact that it does not require dynamic imaging and the fact that identical overlap was obtained when using THK5317 R₁. Abbreviations: DVR, distribution volume ratio; FDG, [¹⁸F]fluorodeoxyglucose; PET, positron emission tomography; p-SUVR, early-frame standardized uptake value ratio; R₁, ratio of tracer delivery in target to reference region; THK5317, [¹⁸F]THK5317; ∩, overlap symbol indicating voxels shared by binarized parametric images.

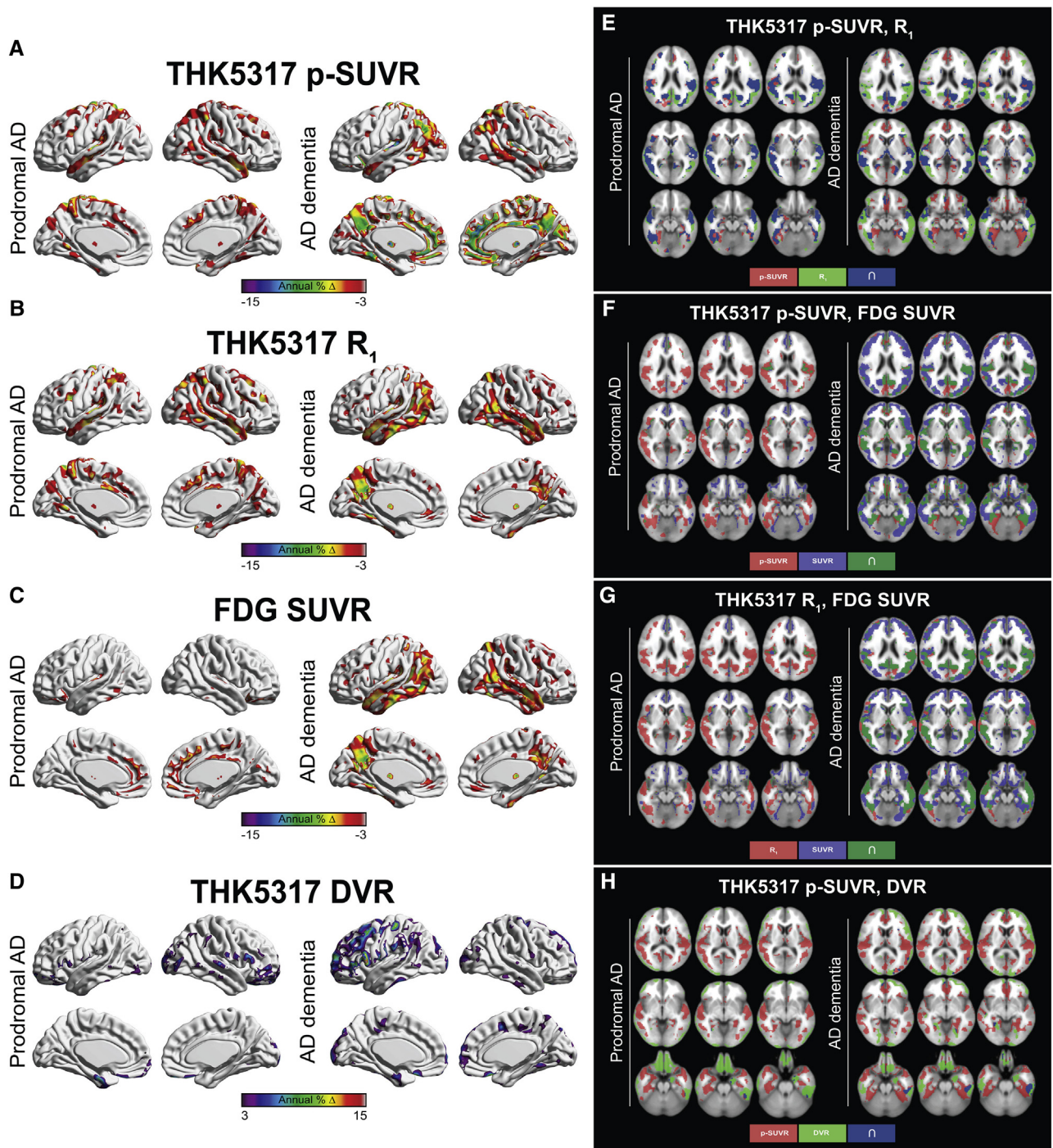


Fig. 4. Subgroup-level annual percentage change maps for perfusion, metabolism, and tau. Surface projection images showing annual percentage change in PET measures in prodromal AD and AD dementia patients: THK5317 p-SUVR (A), THK5317 R₁ (B), FDG SUVR (C), and THK5317 DVR (D). Spatial overlap of annual percentage change images binarized using the average test-retest repeatability of THK5317 perfusion measures is shown in prodromal AD and AD dementia patients for THK5317 perfusion measures (E), THK5317 p-SUVR and FDG SUVR (F), and THK5317 R₁ and FDG SUVR (G). For the overlap between perfusion and THK5317 DVR (H), THK5317 p-SUVR was chosen because of the potentially greater clinical applicability of p-SUVR due to the fact that it does not require dynamic imaging and the fact that identical overlap was obtained when using THK5317 R₁. Images in panels (E–H) are in radiologic orientation. Abbreviations: AD, Alzheimer's disease; DVR, distribution volume ratio; FDG, [¹⁸F]fluorodeoxyglucose; PET, positron emission tomography; p-SUVR, early-frame standardized uptake value ratio; R₁, ratio of tracer delivery in target to reference region; THK5317, [¹⁸F]THK5317; ∩, overlap symbol indicating voxels shared by binarized parametric images.

models were not included in our analyses. The use of such models, particularly with larger sample sizes, would perhaps have proved better suited to characterizing the trajectories of perfusion, metabolism, and tau pathology in AD. Moreover, while FDG SUVR has previously been validated against fully quantitative measures of cerebral glucose metabolic rate, it remains a relative measure only; furthermore, there are as yet no studies validating the use of THK5317 p-SUVR and R_1 against absolute measures of brain perfusion, such as arterial spin labelling MRI or [^{15}O]water PET. Finally, incorporation of markers of vascular pathology would have allowed for the investigation of possible ties between this pathophysiological process and the observed association between perfusion and metabolism.

In conclusion, the partial spatial mismatch between THK5317 perfusion measures and FDG SUVR here observed using longitudinal data may be indicative of an altered parallelism between perfusion and metabolism, possibly due to variation in the spatiotemporal association of the underlying processes as a function of AD disease severity. The complex multifactorial basis of AD, characterized by different effects of A β , tau, glial activation, and neuroinflammation at different stages of disease progression, may underlie the observed variation in the spatiotemporal trajectories of the functional biomarkers investigated in this study. Already incorporated into current thinking about AD biomarker dynamics [48–50], this concept of spatiotemporally offset courses may likewise account for the minimal overlap we observed between changes in functional measures and THK5317 retention. Additional, more adequately powered, longitudinal studies enabling inferential statistics between prodromal and AD dementia stages, as well as more varied diagnostic groups, will be required to expand these findings and, in particular, to delineate the conditions under which THK5317 perfusion measures may prove suitable proxies for FDG PET.

Acknowledgments

This study was funded by the Swedish Research Council (project 05817), the Swedish Foundation for Strategic Research (SSF), the Regional Agreement on Medical Training and Clinical Research (ALF) for Stockholm County Council, the Strategic Research Programme in Neuroscience at Karolinska Institutet, the Foundation for Old Servants, the Axel Linders Foundation, Gun and Bertil Stohne Foundation, the KI Foundations, the Swedish Brain Foundation, the Swedish Alzheimer's Foundation (Alzheimerfonden), Demensfonden, the Wenner-Gren Foundation, KTH-SLL grant, and the EU FW7 large-scale integrating project INMiND (<http://www.unimuenster.de/INMiND>).

Supplementary data

Supplementary data related to this article can be found at <https://doi.org/10.1016/j.jalz.2017.11.008>.

RESEARCH IN CONTEXT

1. Systematic review: Cross-sectional data from the tau-specific positron emission tomography (PET) tracer [^{18}F]THK5317 suggest that [^{18}F]fluorodeoxyglucose PET data can be approximated using perfusion measures (early-frame standardized uptake value ratio and the ratio of tracer delivery in target to reference regions). A single [^{18}F]THK5317 study could thus provide both metabolic and molecular information. The longitudinal relationship between [^{18}F]THK5317 perfusion measures, glucose metabolism, and [^{18}F]THK5317 retention, however, has not been investigated.
2. Interpretation: Our findings suggest a partial uncoupling between perfusion and metabolism, possibly as a function of Alzheimer's disease severity. Further, the limited spatial overlap between longitudinal changes in perfusion and [^{18}F]THK5317 retention suggests that these processes may follow spatiotemporally offset courses.
3. Future directions: Given the possible future clinical use of tau PET, further studies aiming to better delineate the conditions under which [^{18}F]THK5317 perfusion measures may prove suitable proxies for [^{18}F]fluorodeoxyglucose PET are required.

References

- [1] Ishii K, Sasaki M, Yamaji S, Sakamoto S, Kitagaki H, Mori E. Demonstration of decreased posterior cingulate perfusion in mild Alzheimer's disease by means of H215O positron emission tomography. *Eur J Nucl Med* 1997;24:670–3.
- [2] Johnson KA, Mueller ST, Walshe TM, English RJ, Holman BL. Cerebral perfusion imaging in Alzheimer's disease. Use of single photon emission computed tomography and iofetamine hydrochloride I 123. *Arch Neurol* 1987;44:165–8.
- [3] Friedland RP, Budinger TF, Ganz E, Yano Y, Mathis CA, Koss B, et al. Regional cerebral metabolic alterations in dementia of the Alzheimer type: positron emission tomography with [^{18}F]fluorodeoxyglucose. *J Comput Assist Tomogr* 1983;7:590–8.
- [4] Mosconi L, Tsui WH, De Santi S, Li J, Rusinek H, Convit A, et al. Reduced hippocampal metabolism in MCI and AD: automated FDG-PET image analysis. *Neurology* 2005;64:1860–7.
- [5] Nihashi T, Yatsuya H, Hayasaka K, Kato R, Kawatsu S, Arahata Y, et al. Direct comparison study between FDG-PET and IMP-SPECT for diagnosing Alzheimer's disease using 3D-SSP analysis in the same patients. *Radiat Med* 2007;25:255–62.
- [6] Silverman DH. Brain 18F-FDG PET in the diagnosis of neurodegenerative dementias: comparison with perfusion SPECT and with clinical evaluations lacking nuclear imaging. *J Nucl Med* 2004;45:594–607.
- [7] Paulson OB, Hasselbalch SG, Rostrup E, Knudsen GM, Pelligrino D. Cerebral blood flow response to functional activation. *J Cereb Blood Flow Metab* 2010;30:2–14.

- [8] Chen YJ, Rosario BL, Mowrey W, Laymon CM, Lu X, Lopez OL, et al. Relative 11C-PiB delivery as a proxy of relative CBF: quantitative evaluation using single-session 15O-water and 11C-PiB PET. *J Nucl Med* 2015;56:1199–205.
- [9] Rodriguez-Vieitez E, Leuzy A, Chiotis K, Saint-Aubert L, Wall A, Nordberg A. Comparability of [18F]THK5317 and [11C]PIB blood flow proxy images with [18F]FDG positron emission tomography in Alzheimer's disease. *J Cereb Blood Flow Metab* 2017; 37:740–9.
- [10] Gunn RN, Gunn SR, Cunningham VJ. Positron emission tomography compartmental models. *J Cereb Blood Flow Metab* 2001; 21:635–52.
- [11] Logan J, Fowler JS, Volkow ND, Wang GJ, Ding YS, Alexoff DL. Distribution volume ratios without blood sampling from graphical analysis of PET data. *J Cereb Blood Flow Metab* 1996;16:834–40.
- [12] Lammertsma AA, Hume SP. Simplified reference tissue model for PET receptor studies. *Neuroimage* 1996;4:153–8.
- [13] Zhou Y, Resnick SM, Ye W, Fan H, Holt DP, Klunk WE, et al. Using a reference tissue model with spatial constraint to quantify [11C]Pittsburgh compound B PET for early diagnosis of Alzheimer's disease. *Neuroimage* 2007;36:298–312.
- [14] Koeppe RA, Gilman S, Joshi A, Liu S, Little R, Junck L, et al. 11C-DTBZ and 18F-FDG PET measures in differentiating dementias. *J Nucl Med* 2005;46:936–44.
- [15] Rodriguez-Vieitez E, Carter SF, Chiotis K, Saint-Aubert L, Leuzy A, Scholl M, et al. Comparison of early-phase 11C-deuterium-l-deprenyl and 11C-Pittsburgh Compound B PET for assessing brain perfusion in Alzheimer disease. *J Nucl Med* 2016;57:1071–7.
- [16] Rostomian AH, Madison C, Rabinovici GD, Jagust WJ. Early 11C-PIB frames and 18F-FDG PET measures are comparable: a study validated in a cohort of AD and FTLD patients. *J Nucl Med* 2011; 52:173–9.
- [17] Farid K, Hong YT, Aigbirhio FI, Fryer TD, Menon DK, Warburton EA, et al. Early-phase 11C-PiB PET in amyloid angiopathy-related symptomatic cerebral hemorrhage: potential diagnostic value? *PLoS One* 2015;10:e0139926.
- [18] Lemoine L, Saint-Aubert L, Marutle A, Antoni G, Eriksson JP, Ghetti B, et al. Visualization of regional tau deposits using (3)H-THK5117 in Alzheimer brain tissue. *Acta Neuropathol Commun* 2015;3:40.
- [19] Jonasson M, Wall A, Chiotis K, Saint-Aubert L, Wilking H, Spryca M, et al. Tracer kinetic analysis of (S)-18F-THK5117 as a PET tracer for assessing tau pathology. *J Nucl Med* 2016; 57:574–81.
- [20] Garibotto V, Morbelli S, Pagani M. Erratum to: dual-phase amyloid PET: hitting two birds with one stone. *Eur J Nucl Med Mol Imaging* 2016;43:1747.
- [21] Valentina G, Silvia M, Marco P. Dual-phase amyloid PET: hitting two birds with one stone. *Eur J Nucl Med Mol Imaging* 2016;43:1300–3.
- [22] Chiotis K, Saint-Aubert L, Savitcheva I, Jelic V, Andersen P, Jonasson M, et al. Imaging in-vivo tau pathology in Alzheimer's disease with THK5317 PET in a multimodal paradigm. *Eur J Nucl Med Mol Imaging* 2016;43:1686–99.
- [23] Saint-Aubert L, Almkvist O, Chiotis K, Almeida R, Wall A, Nordberg A. Regional tau deposition measured by [18F]THK5317 positron emission tomography is associated to cognition via glucose metabolism in Alzheimer's disease. *Alzheimers Res Ther* 2016;8:38.
- [24] Chiotis K, Saint-Aubert L, Rodriguez-Vieitez E, Leuzy A, Almkvist O, Savitcheva I, et al. Longitudinal changes of tau PET imaging in relation to hypometabolism in prodromal and Alzheimer's disease dementia. *Mol Psychiatry* 2017 May 16. <https://doi.org/10.1038/mp.2017.108>. [Epub ahead of print].
- [25] McKhann GM, Knopman DS, Chertkow H, Hyman BT, Jack CR Jr, Kawas CH, et al. The diagnosis of dementia due to Alzheimer's disease: recommendations from the National Institute on Aging-Alzheimer's Association workgroups on diagnostic guidelines for Alzheimer's disease. *Alzheimers Dement* 2011;7:263–9.
- [26] Petersen RC, Smith GE, Waring SC, Ivnik RJ, Tangalos EG, Kokmen E. Mild cognitive impairment: clinical characterization and outcome. *Arch Neurol* 1999;56:303–8.
- [27] Dubois B, Feldman HH, Jacova C, Hampel H, Molinuevo JL, Blennow K, et al. Advancing research diagnostic criteria for Alzheimer's disease: the IWG-2 criteria. *Lancet Neurol* 2014; 13:614–29.
- [28] Hammers A, Allom R, Koeppe MJ, Free SL, Myers RM, Lemieux L, et al. Three-dimensional maximum probability atlas of the human brain, with particular reference to the temporal lobe. *Hum Brain Mapp* 2003;19:224–47.
- [29] Armstrong MJ, Litvan I, Lang AE, Bak TH, Bhatia KP, Borroni B, et al. Criteria for the diagnosis of corticobasal degeneration. *Neurology* 2013;80:496–503.
- [30] Leenders KL, Perani D, Lammertsma AA, Heather JD, Buckingham P, Healy MJ, et al. Cerebral blood flow, blood volume and oxygen utilization. Normal values and effect of age. *Brain* 1990;113:27–47.
- [31] Rodriguez G, Warkentin S, Risberg J, Rosadini G. Sex differences in regional cerebral blood flow. *J Cereb Blood Flow Metab* 1988; 8:783–9.
- [32] Chiu NT, Lee BF, Hsiao S, Pai MC. Educational level influences regional cerebral blood flow in patients with Alzheimer's disease. *J Nucl Med* 2004;45:1860–3.
- [33] Wierenga CE, Clark LR, Dev SI, Shin DD, Jurick SM, Rissman RA, et al. Interaction of age and APOE genotype on cerebral blood flow at rest. *J Alzheimers Dis* 2013;34:921–35.
- [34] Smailagic N, Vacante M, Hyde C, Martin S, Ukoumunne O, Sachpekidis C. (1)(8)F-FDG PET for the early diagnosis of Alzheimer's disease dementia and other dementias in people with mild cognitive impairment (MCI). *Cochrane Database Syst Rev* 2015; 1:CD010632.
- [35] Kogure D, Matsuda H, Ohnishi T, Asada T, Uno M, Kunihiro T, et al. Longitudinal evaluation of early Alzheimer's disease using brain perfusion SPECT. *J Nucl Med* 2000;41:1155–62.
- [36] Fouquet M, Desgranges B, Landeau B, Duchesnay E, Mezenge F, de la Sayette V, et al. Longitudinal brain metabolic changes from amnesic mild cognitive impairment to Alzheimer's disease. *Brain* 2009; 132:2058–67.
- [37] Pasqualetti G, Harris R, Rinne J, Fan Z, Hinz R, Brooks DJ, et al. Does cerebral glucose metabolism and blood flow dissociate in early stages of Alzheimer's disease? *Alzheimers Dement* 2014;10:P536.
- [38] Quintanilla RA, von Bernhardi R, Godoy JA, Inestrosa NC, Johnson GV. Phosphorylated tau potentiates A β -induced mitochondrial damage in mature neurons. *Neurobiol Dis* 2014; 71:260–9.
- [39] Pascoal TA, Mathotaarachchi S, Mohades S, Benedet AL, Chung CO, Shin M, et al. Amyloid-beta and hyperphosphorylated tau synergy drives metabolic decline in preclinical Alzheimer's disease. *Mol Psychiatry* 2017;22:306–11.
- [40] Merlini M, Wanner D, Nitsch RM. Tau pathology-dependent remodeling of cerebral arteries precedes Alzheimer's disease-related microvascular cerebral amyloid angiopathy. *Acta Neuropathol* 2016; 131:737–52.
- [41] Villemagne VL, Pike KE, Chetelat G, Ellis KA, Mulligan RS, Bourgeat P, et al. Longitudinal assessment of Abeta and cognition in aging and Alzheimer disease. *Ann Neurol* 2011;69:181–92.
- [42] Majerova P, Zilkova M, Kazmerova Z, Kovac A, Paholikova K, Kovacech B, et al. Microglia display modest phagocytic capacity for extracellular tau oligomers. *J Neuroinflammation* 2014;11:161.
- [43] Carter SF, Scholl M, Almkvist O, Wall A, Engler H, Langstrom B, et al. Evidence for astrocytosis in prodromal Alzheimer disease provided by

- ¹¹C-deuterium-L-deprenyl: a multitracer PET paradigm combining ¹¹C-Pittsburgh compound B and ¹⁸F-FDG. *J Nucl Med* 2012;53:37–46.
- [44] Zimmer ER, Parent MJ, Souza DG, Leuzy A, Lecrux C, Kim HI, et al. [¹⁸F]FDG PET signal is driven by astroglial glutamate transport. *Nat Neurosci* 2017;20:393–5.
- [45] Ashraf A, Fan Z, Brooks DJ, Edison P. Cortical hypermetabolism in MCI subjects: a compensatory mechanism? *Eur J Nucl Med Mol Imaging* 2015;42:447–58.
- [46] Braak H, Braak E. Neuropathological stageing of Alzheimer-related changes. *Acta Neuropathol* 1991;82:239–59.
- [47] Ishiki A, Okamura N, Furukawa K, Furumoto S, Harada R, Tomita N, et al. Longitudinal assessment of tau pathology in patients with Alzheimer's disease using [¹⁸F]THK-5117 positron emission tomography. *PLoS One* 2015;10:e0140311.
- [48] Jack CR Jr, Knopman DS, Jagust WJ, Petersen RC, Weiner MW, Aisen PS, et al. Tracking pathophysiological processes in Alzheimer's disease: an updated hypothetical model of dynamic biomarkers. *Lancet Neurol* 2013;12:207–16.
- [49] Jack CR Jr, Wiste HJ, Lesnick TG, Weigand SD, Knopman DS, Vemuri P, et al. Brain beta-amyloid load approaches a plateau. *Neurology* 2013;80:890–6.
- [50] Wirth M, Pichet Binette A, Brunecker P, Kobe T, Witte AV, Floel A. Divergent regional patterns of cerebral hypoperfusion and gray matter atrophy in mild cognitive impairment patients. *J Cereb Blood Flow Metab* 2017;37:814–24.